Supporting Information

Hierarchical iron molybdate nanostructure array for efficient water oxidation through optimizing electron density

Jun-Jun Zhang[a*,1], Chun-Ming Yang[c, 1], Chang-Qing Jin[a], Wei-Wei Bao[b*], Rui-Hua Nan[a], Lin Hu[a], Ge Liu[a], Nan-Nan Zhang[d]

[a]School of Materials Science and Chemical Engineering, Xi'an Technological University, Xi'an, Shaanxi 710021, China.

[b]National & Local Joint Engineering Laboratory for Slag Comprehensive Utilization and Environmental Technology, School of Material Science and Engineering, Shaanxi University of Technology, Hanzhong 723000, Shaanxi, China

[c]Shaanxi Key Laboratory of Chemical Reaction Engineering, College of Chemistry & Chemical Engineering, Yan'an University, Yan'an 716000, China

[d]Instrumental Analysis Center, Shanghai Jiao Tong University, Shanghai 200240, China

[1]These authors contributed equally to this work.

Correspondence to:

E-mail: zhangjunjun@xatu.edu.cn (J. J. Zhang); baowei1834@163.com (W.W. Bao).

List of Contents

1. Experimental Section

1.1 Materials

Iron(Ⅱ) chloride tetrahydrate ($FeCl_2 \cdot 4H_2O$), Sodium molybdate dihydrate ($Na_2MoO_4 \cdot 2H_2O$), Iridium(IV) Oxide (IrO_2), and Nafion (5 wt%) were purchased from Shinopharm Chemical Reagent Co. Ltd. Milli-Q ultrapure water was used for all experiments. All chemicals were analytical grade and used as received without further purification.

1.2. Preparation of Ni@$FeMoO_4$ electrode

The nickel foam was treated by ultrasonication in diluted HCl solution for 30 min to remove the surface impurity and cleaned with deionized and ethanol water, respectively. $FeCl_2 \cdot 4H_2O$ (1.8 mmol) and $Na_2MoO_4 \cdot 2H_2O$ (1.8 mmol) were dissolved in 45 mL distilled water. After gentle stirring for 30 min, the clear solution was transferred to a 50 mL Teflon-lined stainless steel autoclave. The washed Ni substrate (3*1 cm) was immersed into the reaction solution. The autoclave was maintained at 120 ^{o}C for 24 h. After the autoclave cooled down at room temperature, the Ni@$FeMoO_4$ electrode was washed with water and ethanol several times, followed by drying at 80 ^{o}C for 10 h.

1.3. Preparation of IrO_2 electrode

To prepare IrO_2 loaded electrodes, 3.6 mg IrO_2 and 20 μL 5 wt% Nafion solution were dispersed in 100 μL 3:7 water/ethanol solvent. The mixture was ultrasonicated for about 1 h to form a homogeneous ink. Then, the catalyst ink was loaded on a preprocessed Ni foam (1*1 cm^2). The loading amount of the catalysts was 3.6 mg cm^{-2}. A similar method was used to prepare Ni+$FeMoO_4$ electrode.

1.4 Material characterizations

The X-ray diffraction (XRD) patterns were recorded on a Bruker D8 Advance X-ray diffractometer with Cu-Kα radiation (λ = 1.5418 Å) with a scan rate of 6° min^{-1}. The SEM measurements were performed on ascanning electron microscope (FESEM, JSM-7610F, 10 kV). The TEM and HRTEM measurements were taken with a JEOL JEM-F200 microscope operated. The samples were prepared by dropping ethanol dispersion of samples onto carbon-coated copper TEM grids using pipettes and dried under ambient condition. The X-ray photoelectron spectroscopy (XPS) measurements were conducted on a Kratos Axis Ultra DLD spectrometer.

1.5 Electrochemical characterizations

Electrochemical measurements are performed with a CHI 730C electrochemistry workstation (CH Instruments, Inc., Shanghai) in a standard three-electrode system. The three-electrode electrochemical cell was consisted of a Ni@$FeMoO_4$, a graphite carbon rod and a

mercury oxide electrode (Hg/HgO) served as working electrode, counter electrode, and reference electrode, respectively. Potentials are reported versus the reversible hydrogen electrode (RHE). All potentials were calculated with respect to RHE via the following equation: ERHE = $E_{Hg/HgO}$ + 0.059pH + 0.098 V. Polarization curves measurements were conducted in 1.0 M KOH solution with a scan rate of 10 mV s^{-1}. The long-term durability test was performed using chronoamperometric measurements. Converted to a RHE according to test correction, the overpotential η was calculated according to formula $\eta = E_{RHE} - 1.23$. The cyclic voltammogram (CV) 500 cycles durability test was conducted by potential cycling from 0.2 to 1.8 V vs. RHE. The polarization curves were establish as overpotential vs log current (log j) to get Tafel plots for evaluating the OER reaction kinetics of obtained catalysts. By fitting the Tafel plots (the linear portion) to the Tafel equation ($\eta = b\log(j) + a$), the Tafel slope can be obtained. To reflect the real catalytic currents, all corresponding polarization curves shown in this paper were calibrated after i*Rs correction. E corrected = E measured – i*Rs (where Ecorr is the i*Rs-compensated potential, Emea is the experimentally measured potential, and Rs is the solution resistance, respectively). The turnover frequency (TOF) is defined as the number of H_2 or O_2 molecules generated per site per second: TOF = j/(n*F*N), where j is the measured current density (A cm^{-2}), n is the mole number of electrons per mole of O_2, F is the Faraday constant (96,485 C mol^{-1}), and N is the content of the catalyst (mol cm^{-2}). Electrochemical impedance spectroscopy (EIS) is a common method for investigating the as-constructed electron transfer kinetics in the OER. The EIS measurements for the Ni@$FeMoO_4$ were performed in 1.0 M KOH using a graphite rod as the counter electrode with the frequency range from 100 KHz to 0.1 Hz. All measurements were conducted at room temperature.

1.6 DFT calculation

All the calculations were performed with the Vienna Ab initio Simulation Package (VASP) based on the density-functional theory (DFT). The generalized gradient approximation (GGA) with PBE functional was used for the differential charge density, and a plane-wave expansion for the basis set with a cutoff energy of 450 eV was employed. $FeMoO_4$ (110) and Ni (111) were used to construct dual interface. Geometry optimizations and differential charge density were performed with a convergence threshold of 10^{-7} eV in energy and 0.05 eV $Å^{-1}$ for the force, respectively. A vacuum of 15 Å along the z-direction was used, which was large enough to minimize the interaction between periodic images (ref. Chem. Commun., 2020,56, 6834; Angew. Chem. Int. Ed. 2018, 57, 2697.).

2. Supplementary Figures:

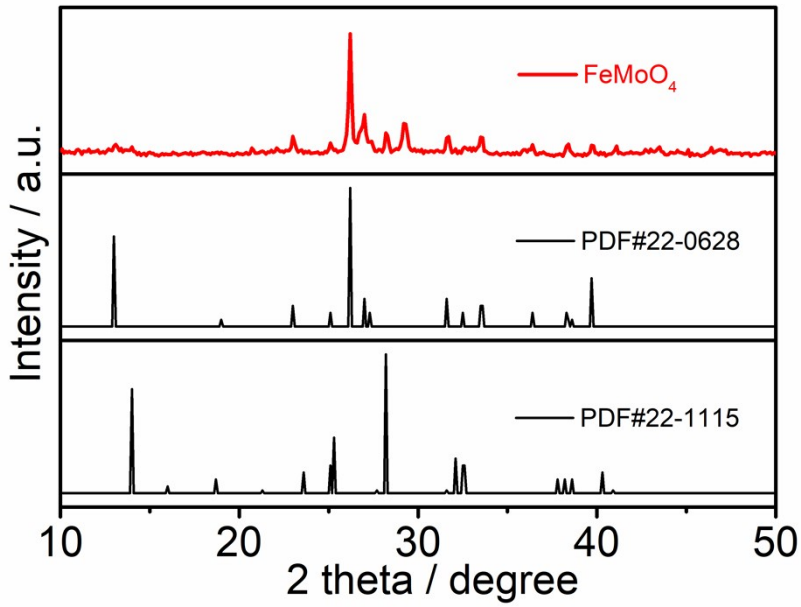

Figure S1. The XRD spectra of $FeMoO_4$ sample.

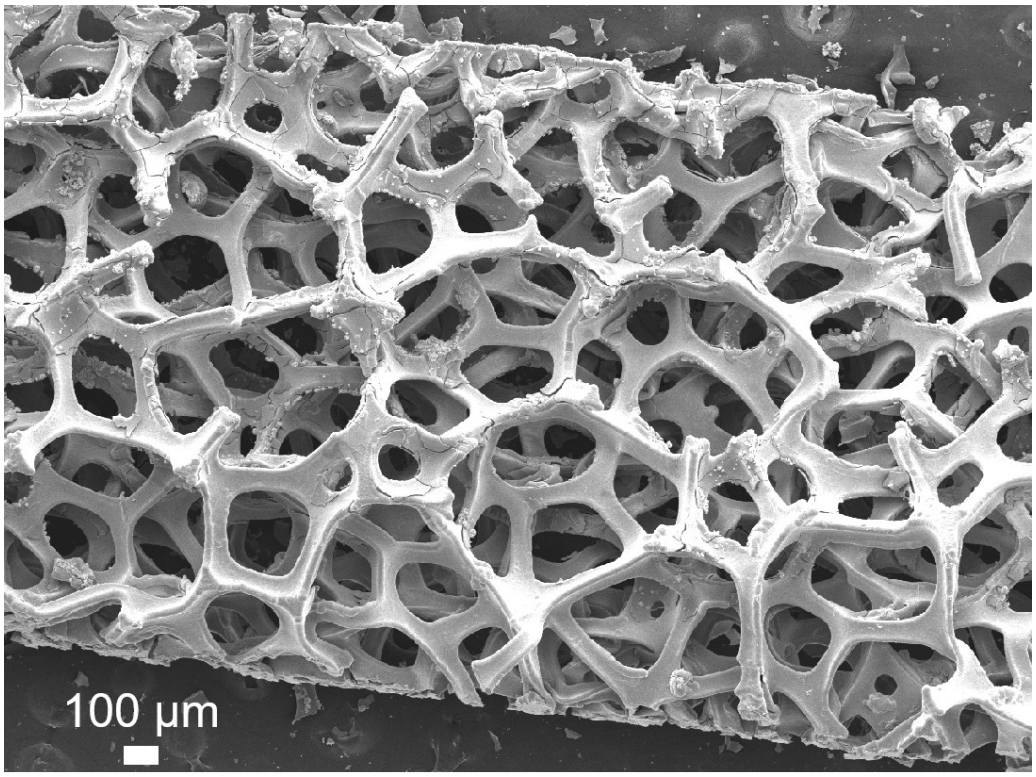

Figure S2. The SEM image of Ni@$FeMoO_4$ sample.

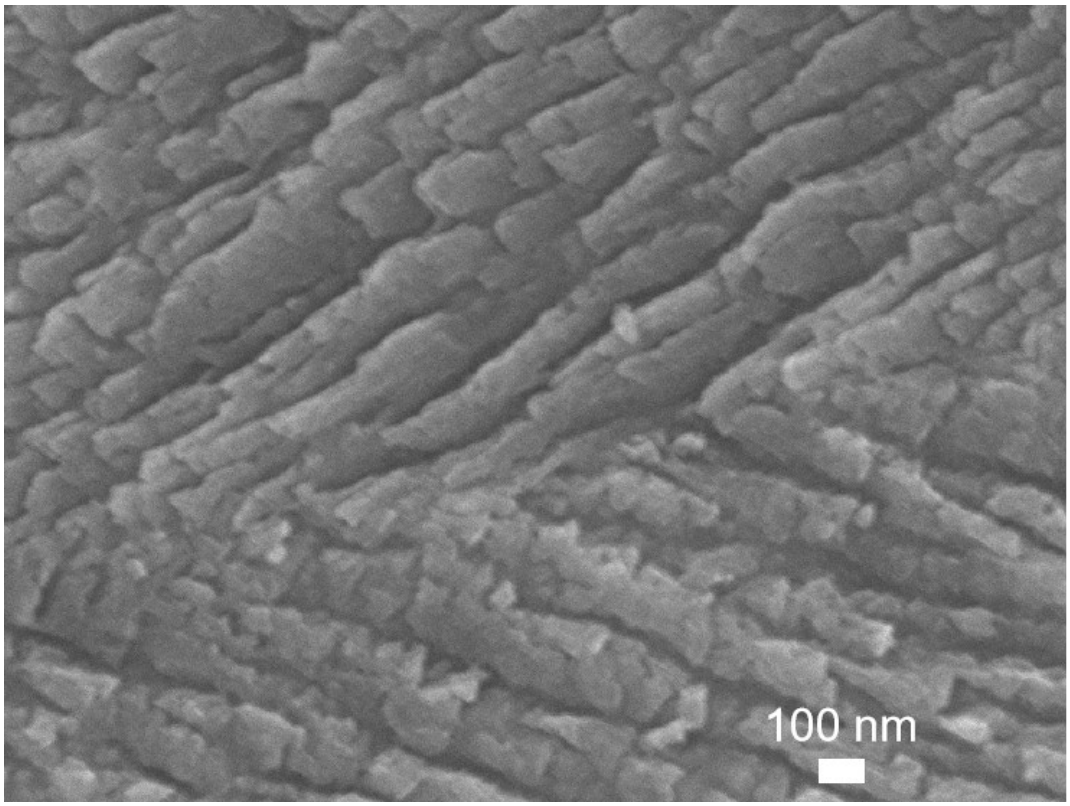

Figure S3. The high-magnification SEM image of Ni@$FeMoO_4$ sample.

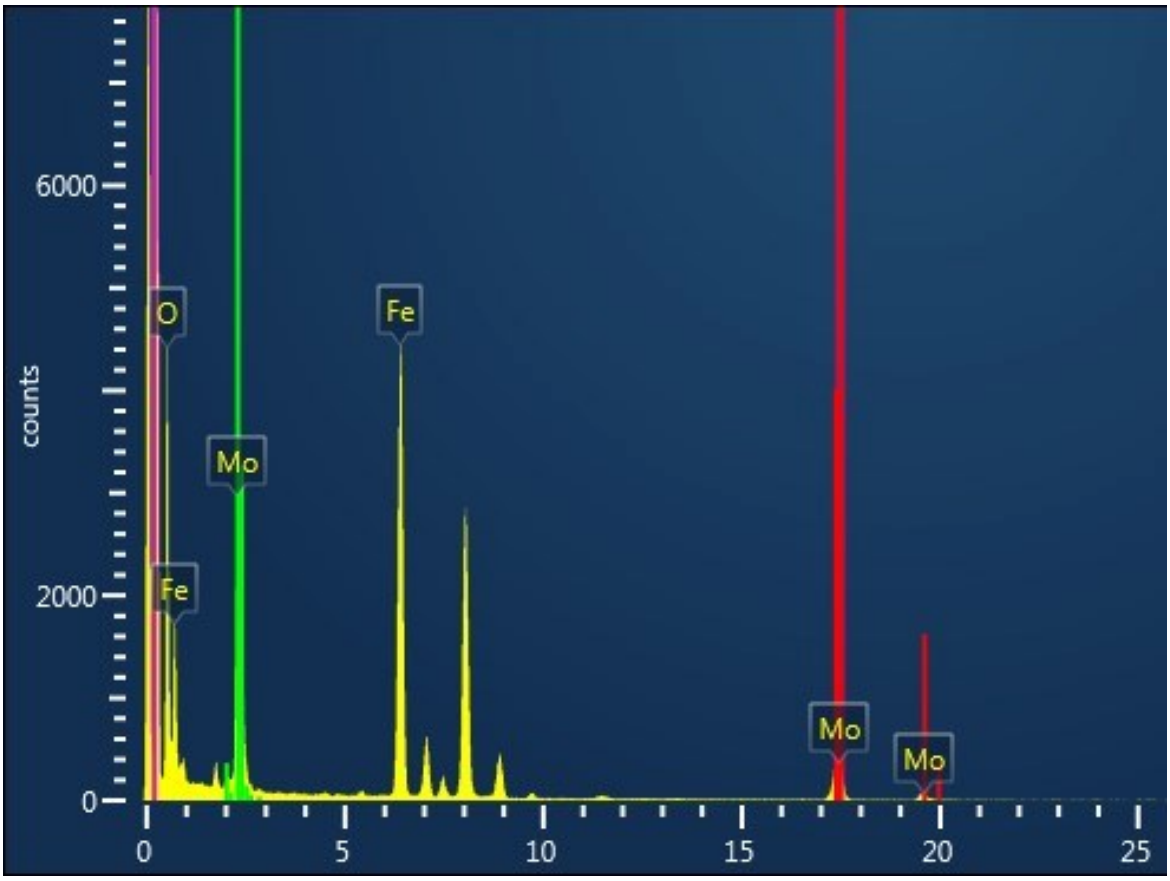

Figure S4. The EDS image of $FeMoO_4$ sample.

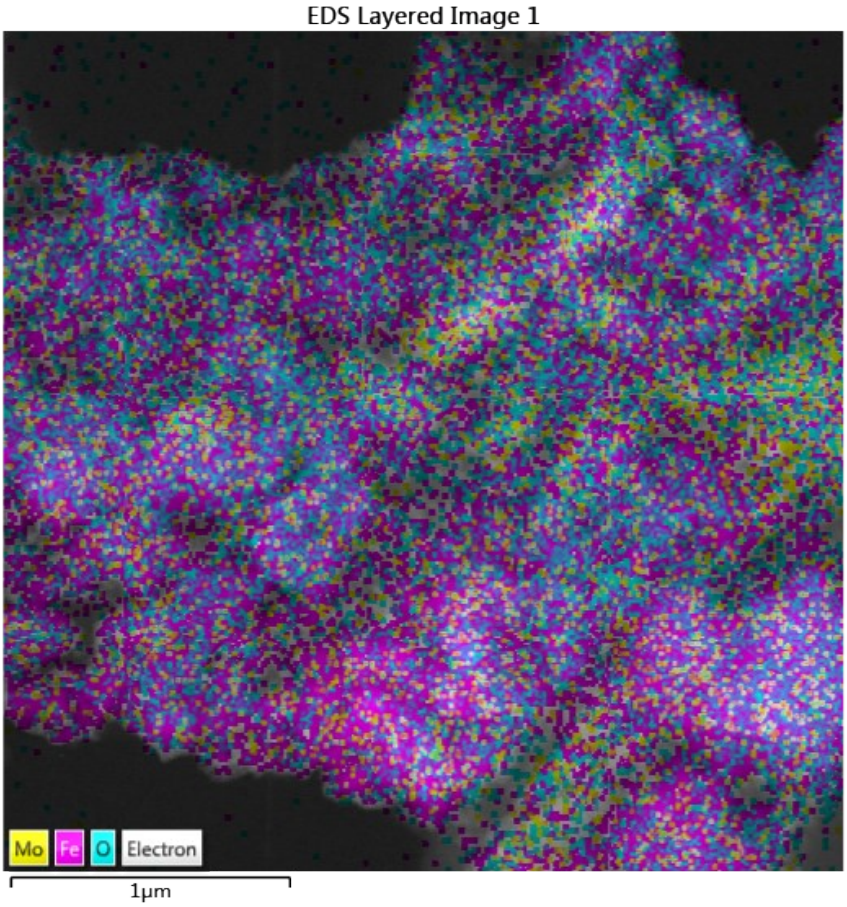

Figure S5. The elemental mapping image of $FeMoO_4$ sample.

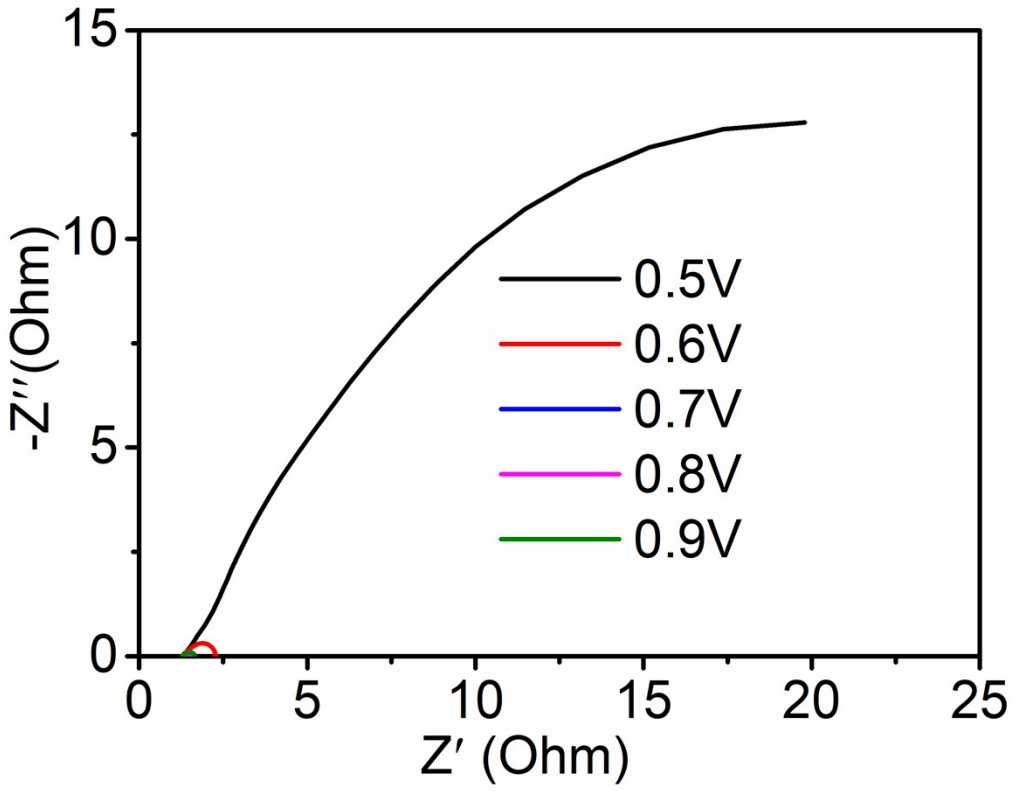

Figure S6. The EIS of the Ni@$FeMoO_4$ electrodes.

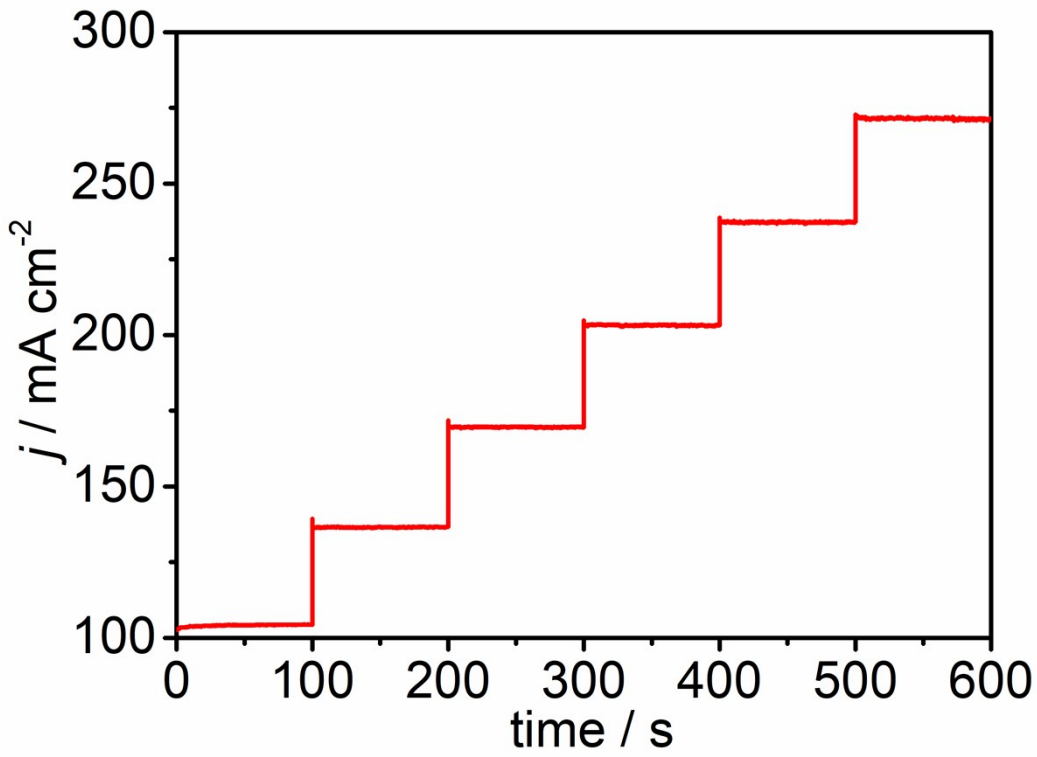

Figure S7. The multi-potential steps of the Ni@$FeMoO_4$ electrodes.

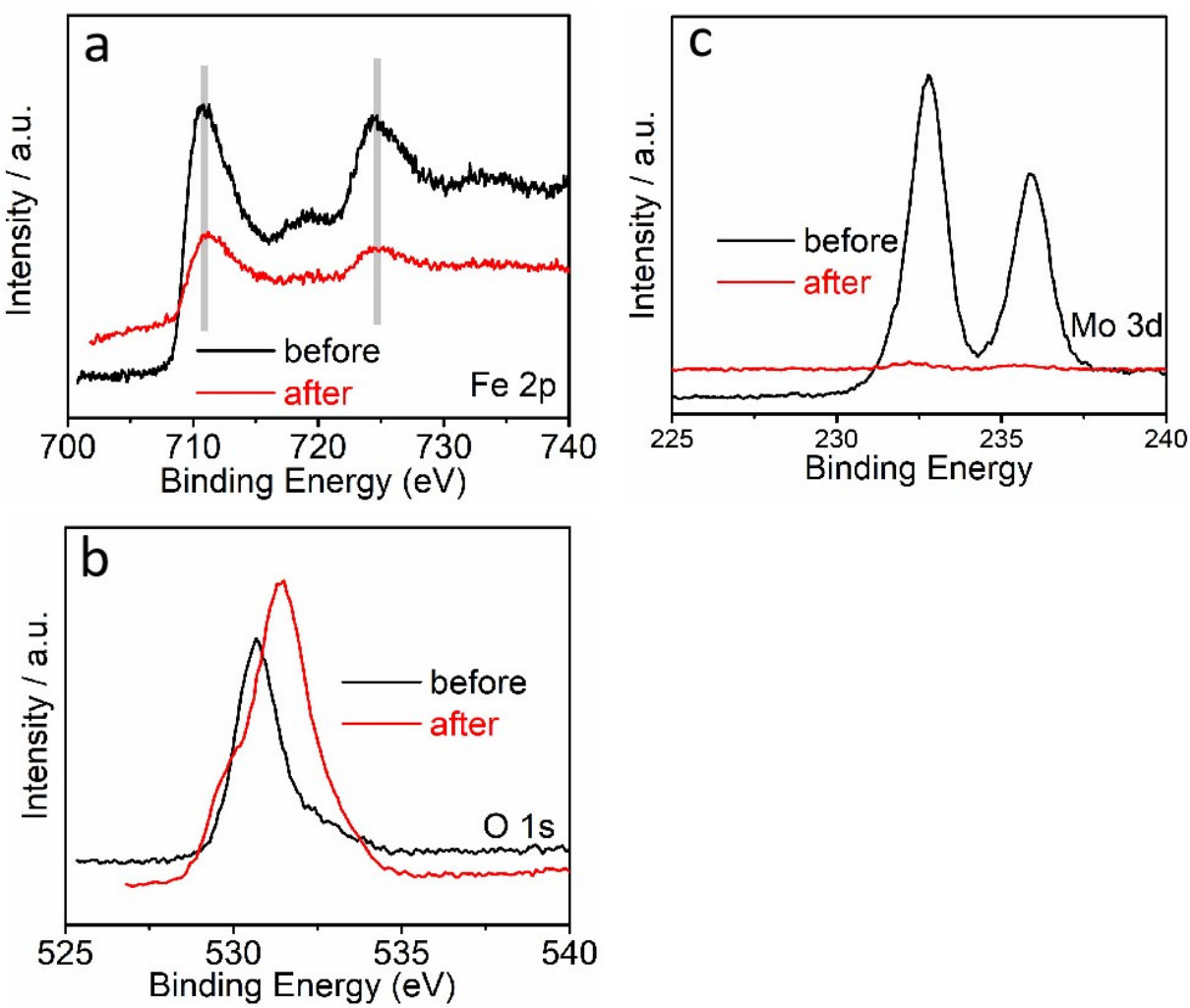

Figure S8. The high-resolution (a) Fe 2p, (b) O 1s, (c) Mo 3d XPS spectra of the $FeMoO_4$ electrode before and after OER.

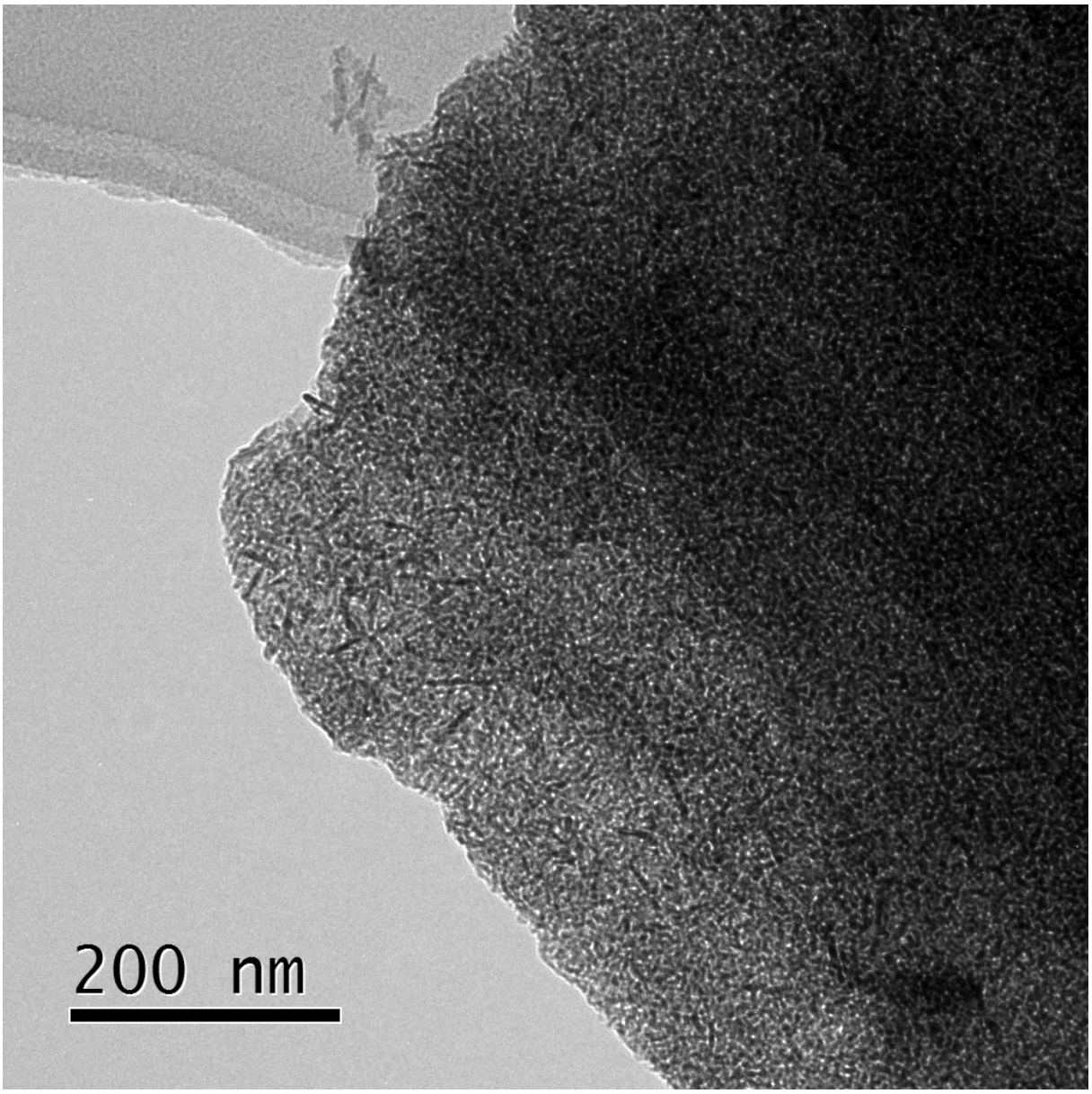

Figure S9. The TEM image of Ni@$FeMoO_4$ electrodes after OER.

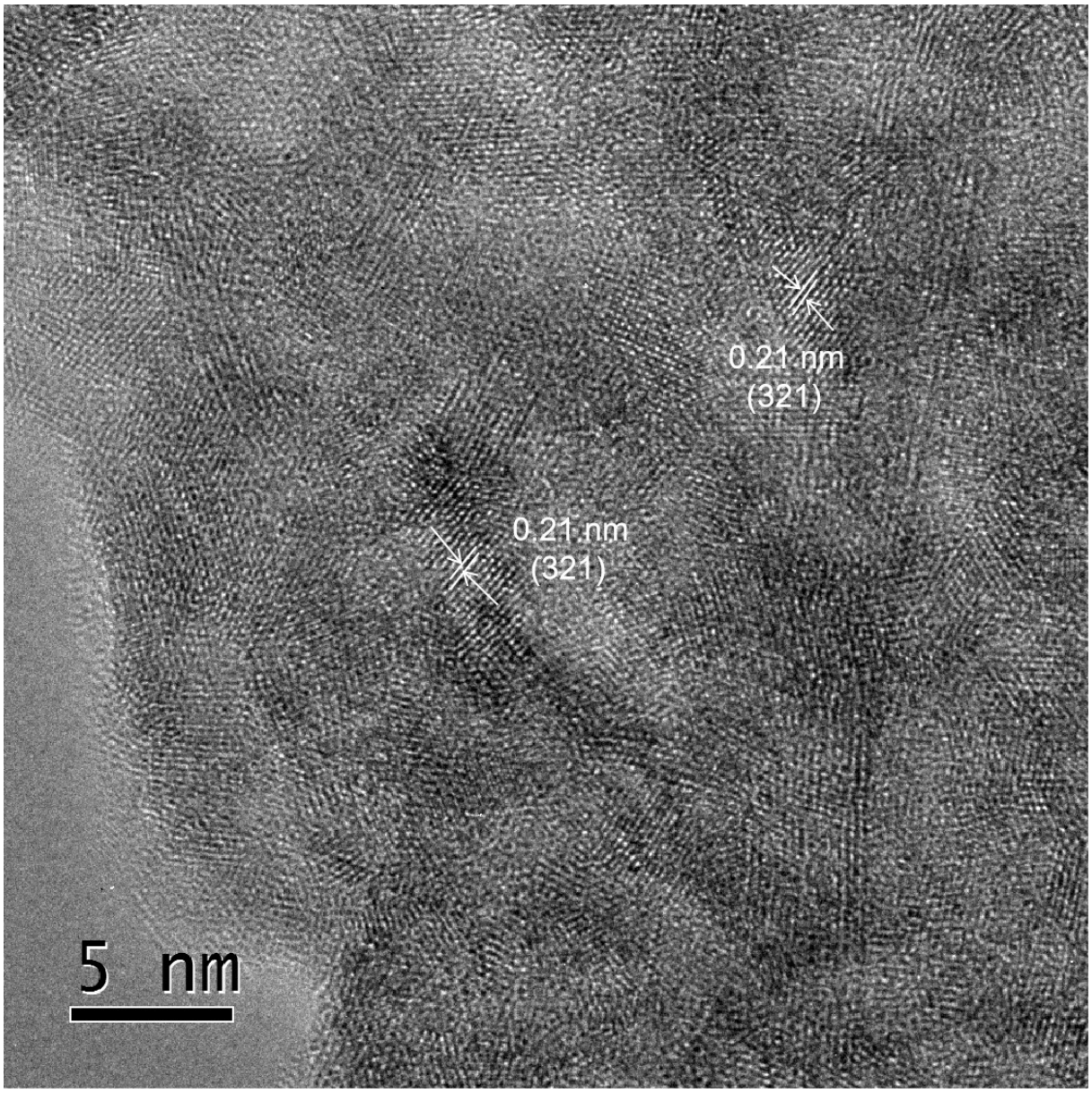

Figure S10. The HR-TEM image of Ni@$FeMoO_4$ electrodes after OER.

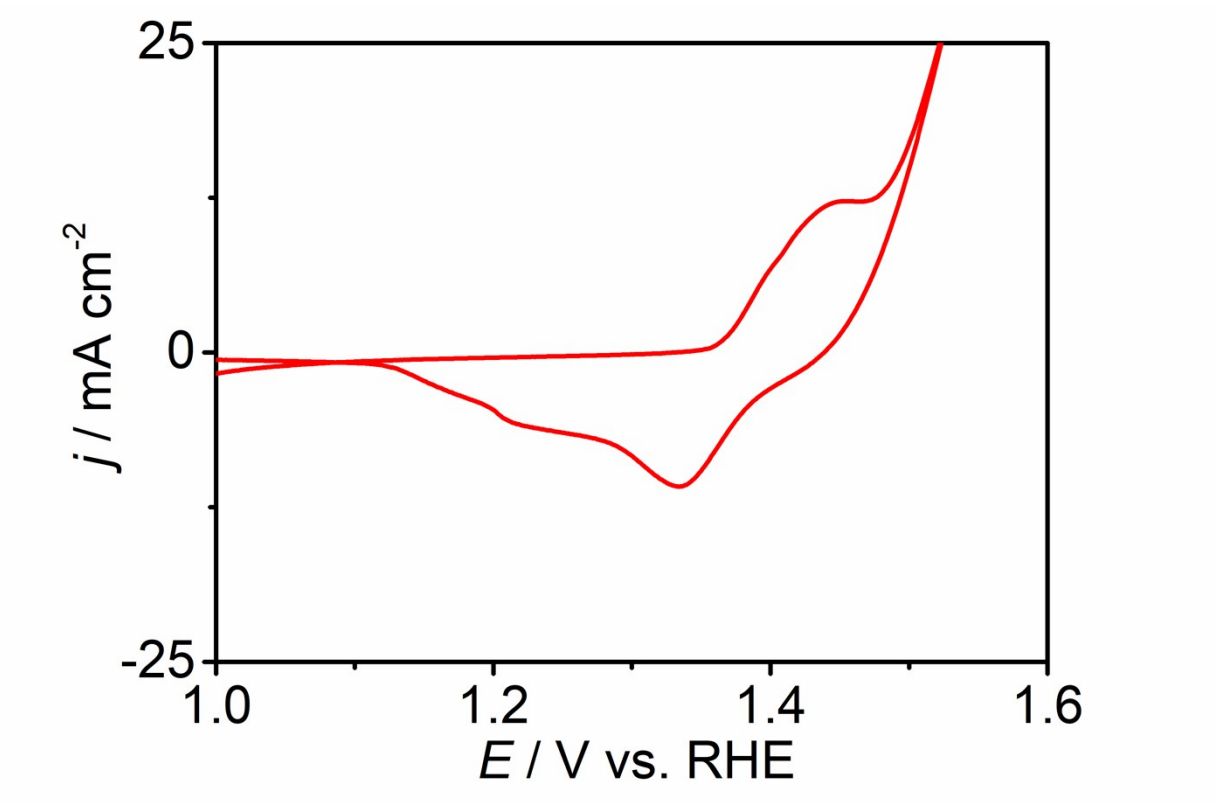

Figure S11. The CV of Ni@$FeMoO_4$ electrodes.

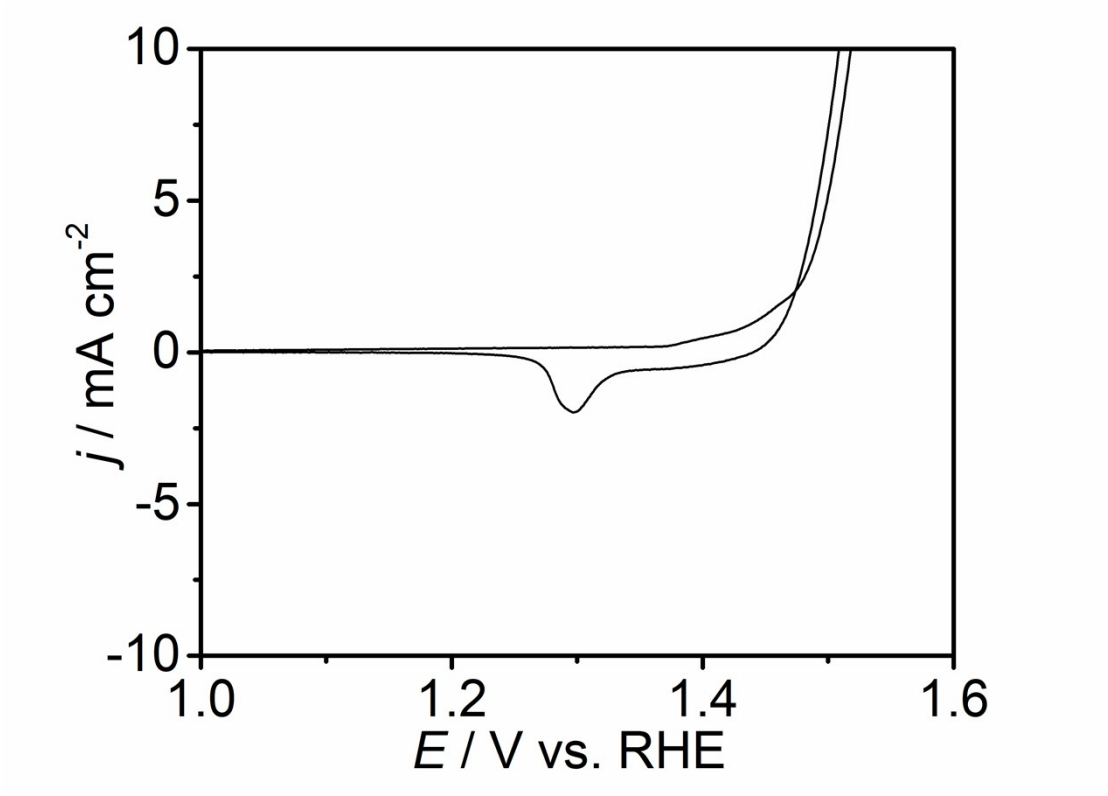

Figure S12. The CV of Ni+$FeMoO_4$ electrodes.

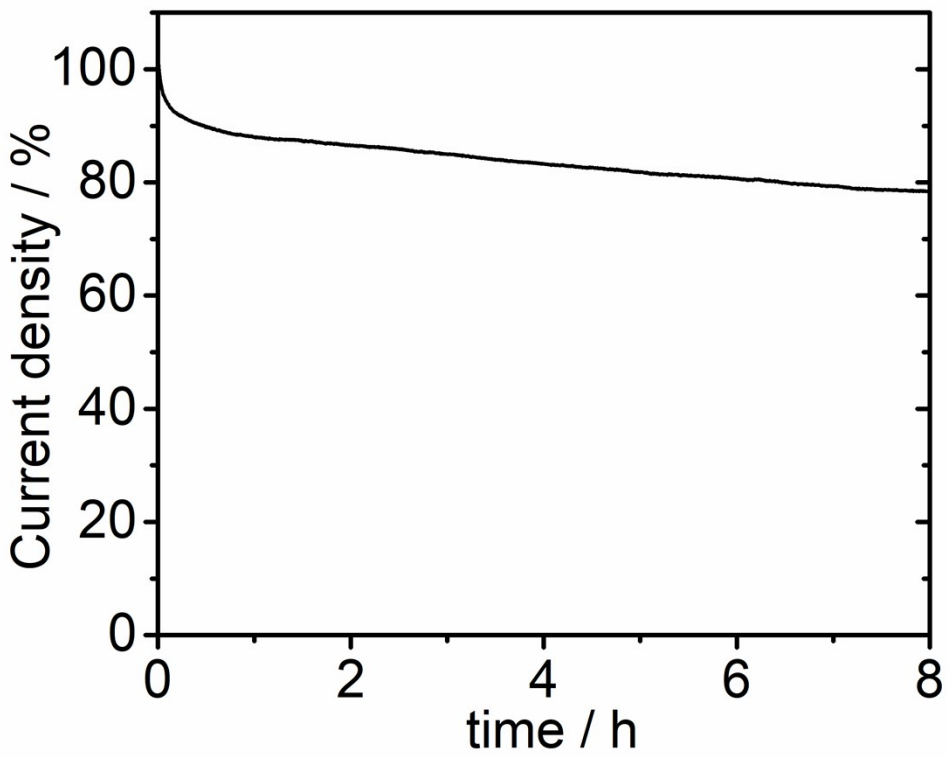

Figure S13. The i-t stability measurement of Ni+$FeMoO_4$ electrode.

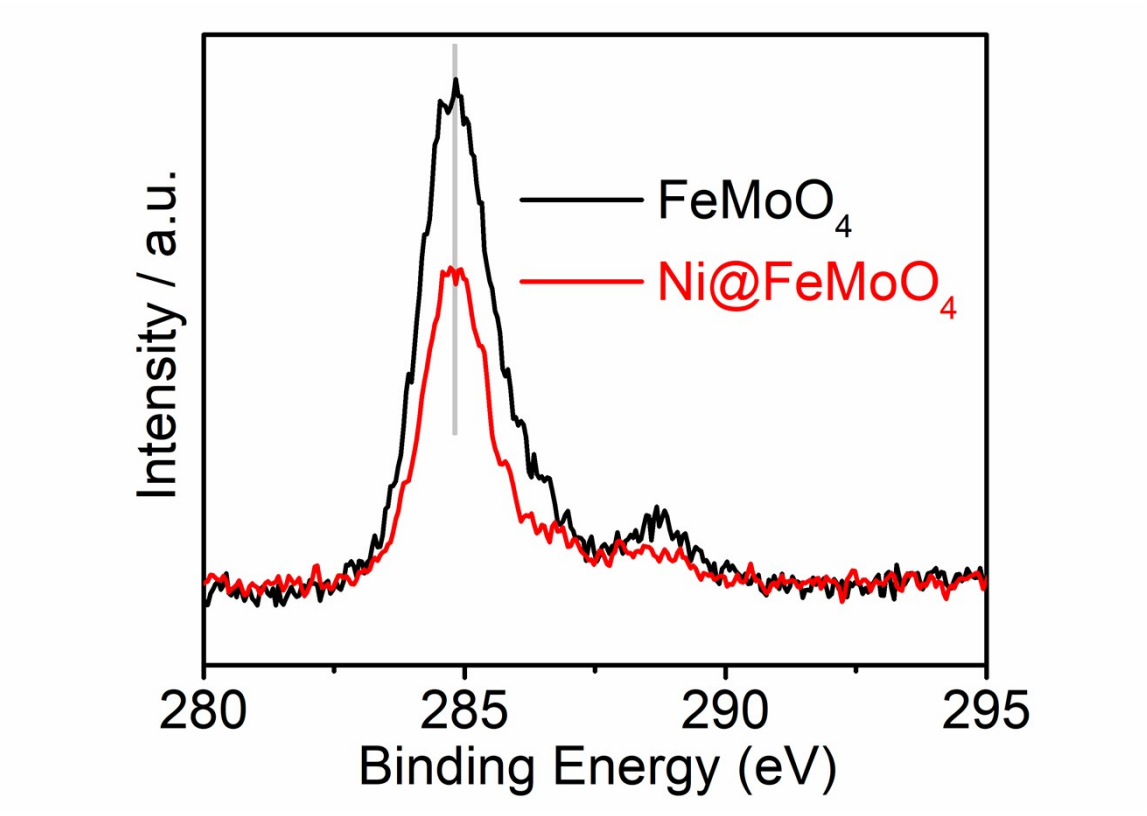

Figure S14. High-resolution C 1s XPS spectra of Ni@$FeMoO_4$ and $FeMoO_4$ sample.

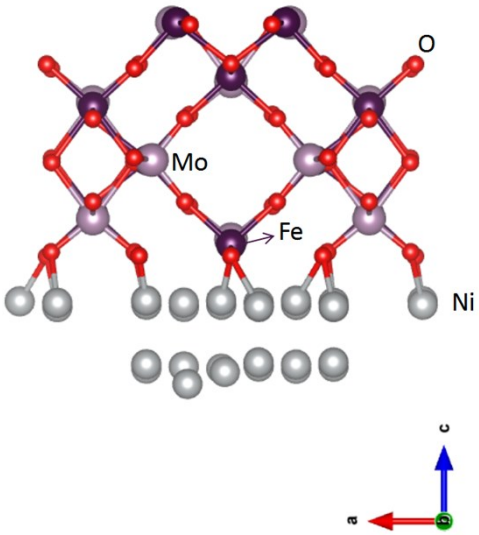

Figure S15. The model unit of a Ni@$FeMoO_4$ catalyst.

3. Supplementary Tables

Table S1. Comparison of the OER performance of NF/FeOOH catalyst with other reported OER catalysts

Catalyst	Loading (mg cm^{-2})	Tafel slope (mV dec-1)	j (mA cm-2)	Overpotential / mV	Reference
Ni@$FeMoO_4$	3.6	**56**	**10**	**177**	**This work**
			50	**276**	
			100	**293**	
			200	**312**	
Fe_2B	0.25	30	10	240	1.J. Mater. Chem. A, 2020,8, 13638-13645
Ni2P/FeP	0.27	43	10	211	2.J. Mater. Chem. A, 2020，
CoFe-LDH/MXene	0.0016	50	10	319	3..Materials Today Energy 12 (2019) 453-462
CoFe LDH	0.2	83	10	300	4.ChemPlusChem 2017, 82,483 –488
$Fe_{0.2}Ni_{0.8}B$/SSG	-----	31.4	30	263	5.Int J Hydrogen Energy，2019， DOI: 10.1016/j.ijhydene.2020.07.171
Co-Ni-P/MoS_2	-----	71	10	235	6.J. Mater. Chem. A, 2020，
CoFeCr hydroxides		40.1	10	260	7.Sustainable Energy Fuels, 2020,4, 3647-3653
$Co_2Mo_3O_8$	0.14	87.5	10	241	8.Angew. Chem. Int. Ed. 2020, DOI: 10.1002/anie.202004533
Au-Ir	0.02	36.9	10	245	9.Nat. Commun. 2020， DOI:10.1038/s41467-020-15391-w
Fe-Co/carbon fiber papers	2	34	10	283	10.Nano Energy 2017, 38 576-584
NiFe@NC	0.2	56	10	350	11.Nano Energy, 2016, 30, 426-433
Porous monolayer NiFe LDH	0.35	47	10	230	12.Adv. Energy Mater. 2019, 9: 1900881.
Ag/CoFe-AN	---	34	10	187	13.*PNAS, 2020, DOI: 10.1073/pnas.2009180117*
Ultrafine monolayer NiFe LDH	0.35	32	10	254	14.Adv. Energy Mater. 2018, 8: 1703585
Ni $Se_{0.5}S_{0.5}$	2.4	61	10	257	15.Adv. Mater., 2020,32, 2000231
CoP-MNA	6.2	65	10	290	16.Adv. Funct. Mater. 2015, 25, 7337-7347.
H_2O-plasma exfoliated CoFeLDHs	0.306	36	10	278	17.Adv. Mater. 2017, 29, 1701546
$Co_3O_{3.87}F_{0.13}$	0.072	56	10	430	18.Applied Catalysis B: Environmental 281 (2021) 119535

cat.-51.9	-----	47.8	30	293.2	19.Adv. Mater. 2020, 32,2001136
NiCoP/CC	2	65	10	242	20. ACS Catal. 2017, 7, 6, 4131–4137
NiFeCr/NF	----	36	onset	240	21.Energy Environ. Sci., 2020, DOI: 10.1039/D0EE01609H.
$CaMoO_4$	2.38	80	50	345	22 Chem. Commun., 2018,54, 5066-5069
3% Au-Ni	1.96	85.3	100	377	23.Chem. Commun., 2020, DOI: 10.1039/D0CC06337A

Notes and references

1. Yinlong Zhu, Qian Lin, Yijun Zhong, Hassan A. Tahini, Zongping Shao, Huanting Wang, Metal Oxide-Based Materials as an Emerging Family of Hydrogen Evolution Electrocatalysts, *J. Mater. Chem. A*, 2020,8, 13638-13645.

2. Dongxu Yang, Zhe Su, Yuanfu Chen, Yingjiong Lu, Bo Yu, Katam Srinivas, Bin Wang Wanli Zhang, Double-shelled hollow bimetallic phosphide nanospheres anchored on nitrogen-doped graphene for boosting water electrolysis, *J. Mater. Chem. A*, 2020, https://doi.org/10.1039/D0TA06766K

3. Chongyan Hao, Yang Wu, Yajing An, Baihua Cui, Jiannan Lin, Xiaoning Li, Dianhui Wang, Minhong Jiang, Zhenxiang Cheng, Shi Hu, Interface-coupling of CoFe-LDH on MXene as high-performance oxygen evolution catalys, *Materials Today Energy* 12 (2019) 453-462

4. Lanxiang Feng, Airong Li, YuxuanLi, Jia Liu, Leidanyang Wang, Liey uan Huang,Yong Wang, and Xingbo Ge, AHighly Active CoFe Layered Double Hydroxide for Water Splitting, ChemPlusChem 2017, 82,483-488

5. Jie Lao; Dong Li; Chunli Jiang; Rong Luo; Hui Peng; Ruijuan Qi; Hechun Lin; Rong Huang; Geoffrey I.N. Waterhouse; Chunhua Luo, Efficient overall water splitting using nickel boride-based electrocatalysts,International Journal of Hydrogen Energy, 2020, DOI: 10.1016/j.ijhydene.2020.07.171

6. J. Bao, Y. Zhou, Y. Zhang, X. Sheng, Y. Wang, S. Liang, C. Guo, W. Yang, T. Zhuang and Y. Hu, J. Mater. Chem. A, 2020, DOI: 10.1039/D0TA07953G.

7.Yibin Yang,Xun Cui, Di Gao, Huichao He, Yingqing Ou, Ming Zhou, Qingxin Lai, Xijun Wei, Peng Xiao and Yunhuai Zhang, Trimetallic CoFeCr hydroxide electrocatalysts synthesized at low temperature for accelerating water oxidation via tuning electronic structure of active sites, *Sustainable Energy Fuels*, 2020,4, 3647-3653

8.Zhao-Qing Liu, Ting Ouyang, Xiao-Tong Wang, Xiu-Qiong Mai, An-Na Chen, Zi-Yuan Tang. Coupling Magnetic Single-Crystal Co2Mo3O8 with Ultrathin Nitrogen-Rich Carbon Layer for Oxygen Evolution Reaction. *Angew. Chem. Int. Ed.* 2020, 132, 12026-12055.

9.Ran Du, Jinying Wang, Ying Wang, René Hübner, Xuelin Fan, Irena Senkovska, Yue Hu, Stefan Kaskel, Alexander Eychmüller. Unveiling reductant chemistry in fabricating noble metal aerogels for superior oxygen evoution and ethanol oxidation. *Nat Commun* 11, 1590 (2020).https://doi.org/10.1038/s41467-020-15391-w.

10.Wanglian Liu, Kuangzhou Du, Lu Liu, Jinxuan Zhang, Zhiwei Zhu, Yuanhua Shao, Meixian Li, One-step electroreductively deposited iron-cobalt composite films as efficient bifunctional electrocatalysts for overall water splitting, *Nano Energy* 38 (2017) 576-584

11.Zhengping Zhang, Yeshen Qin, Meiling Dou, Jing Ji, Feng Wang. One-step conversion from Ni/Fe polyphthalocyanine to N-doped carbon supported Ni-Fe nanoparticles for highly efficient water splitting. *Nano Energy*, 2016, 30, 426-433.

12. X. Zhang, Y. F. Zhao, Y. X. Zhao, R. Shi, G. I. N. Waterhouse and T. R. Zhang, A Simple Synthetic Strategy toward Defect-Rich Porous Monolayer NiFe-Layered Double Hydroxide Nanosheets for Efficient Electrocatalytic Water Oxidation, *Adv. Energy Mater.*, 2019, 9, 1900881

13.Juzhe Liu, Qi Hu, Yu Wang, Zhao Yang, Xiaoyu Fan, Li-Min Liu, and Lin Guo, Achieving delafossite analog by in situ electrochemical self-reconstruction as an oxygen-evolving catalyst,*PNAS*, 2020, DOI: 10.1073/pnas.2009180117, www.pnas.org/cgi/doi/10.1073/pnas.2009180117

14.Y. F. Zhao, X. Zhang, X. D. Jia, G. I. N. Waterhouse, R. Shi, X. R. Zhang, F. Zhan, Y. Tao, L. Z. Wu, C. H. Tung, D. O'Hare and T. R. Zhang, Sub-3 nm Ultrafine Monolayer Layered Double Hydroxide Nanosheets for Electrochemical Water Oxidation, *Adv. Energy Mater.*, 2018, 8, 1703585

15.Yang Wang, Xiaopeng Li, Mengmeng Zhang, Yuanguang Zhou, Dewei Rao, Cheng Zhong, Jinfeng Zhang, Xiaopeng Han, Wenbin Hu, Yucang Zhang, Karim Zaghib, Yuesheng Wang, and Yida Deng, Lattice‐Strain Engineering of Homogeneous $NiS_{0.5}Se_{0.5}$ Core‐Shell Nanostructure as a Highly Efficient and Robust Electrocatalyst for Overall Water Splitting. *Adv. Mater.*, 2020, 2000231, DOI: 10.1002/adma.201900231

16.Y. P. Zhu, Y. P. Liu, T. Z. Ren, Z. Y. Yuan, Self-supported cobalt phosphide mesoporous nanorod arrays: a flexible and bifunctional electrode for highly active electrocatalytic water reduction and oxidation, *Adv. Funct. Mater.*, 2015, 25 (47), 7337-7347.

17. Rong Liu, Yanyong Wang , Dongdong Liu, Yuqin Zou , Shuangyin Wang, Water-Plasma-Enabled Exfoliation of Ultrathin Layered Double Hydroxide Nanosheets with Multivacancies for Water Oxidation, *Adv. Mater.* 2017, 29, 1701546

18. Huiyan Zeng, M'hamed Oubla,Xuepeng Zhong,Nicolas Alonso-Vante, Fei Du,Yu Xie,Yunhui Huang, Jiwei Ma,Rational defect and anion chemistries in Co3O4 for enhanced oxygen evolution reaction, *Applied Catalysis B: Environmental* 281 (2021) 119535

19. Xiong Liu, Ruiting Guo, Kun Ni, Fanjie Xia, Chaojiang Niu, Bo Wen, Jiashen Meng, Peijie Wu, Jinsong Wu, Xiaojun Wu, and Liqiang Mai, Reconstruction-Determined Alkaline Water Electrolysis at Industrial Temperatures, *Adv. Mater.* 2020, 32, 2001136
20. Cheng Du, Lan Yang, Fulin Yang, Gongzhen Cheng, and Wei Luo, Nest-like NiCoP for Highly Efficient Overall Water Splitting, *ACS Catal*. 2017, 7, 6, 4131 – 4137
21. X. Bo, R. K. Hocking, S. Zhou, Y. Li, X. Chen, J. Zhuang, Y. Du and C. Zhao, Capturing the Active Sites of Multimetallic (Oxy)Hydroxides for Oxygen Evolution Reactions, *Energy Environ. Sci.*, 2020, DOI: 10.1039/D0EE01609H.
22. Ying Gou, Qin Liu, Xifeng Shi, Abdullah M. Asiri, Jianming Hu and Xuping Sun, $CaMoO_4$ nanosheet arrays for efficient and durable water oxidation electrocatalysis under alkaline conditions,*Chem. Commun.*, 2018,54, 5066-5069.
23. Wei Gao, Min Lei, Lanqing Li, Dan Wen, Promoting the electrocatalytic property of nickel aerogel by gold decoration for efficient electrocatalytic oxygen evolution in alkali, Chem. Commun., 2020, DOI: 10.1039/D0CC06337A.